*MRS Communications (2015)*, *5*, 519–524
© Materials Research Society, 2015
doi:10.1557/mrc.2015.58

MRS Communications

Research Letter

# Energetics of substituted polyhedral oligomeric silsesquioxanes: a DFT study

**Abu Asaduzzaman,** Materials Science and Engineering, University of Arizona, Tucson, AZ 85721, USA
**Keith Runge,** Materials Science and Engineering, University of Arizona, Tucson, AZ 85721, USA; Quantum Theory Project, University of Florida, Gainesville, FL 32611, USA
**Krishna Muralidharan,** and **P.A. Deymier,** Materials Science and Engineering, University of Arizona, Tucson, AZ 85721, USA
**Lianyang Zhang,** Civil Engineering and Engineering Mechanics, University of Arizona, Tucson, AZ 85721, USA
Address all correspondence to Abu Asaduzzaman at **asaduzzaman@email.arizona.edu**

(Received 26 March 2015; accepted 16 July 2015)

## Abstract

First principles density functional theory calculations were conducted to investigate the structures and energetics of polyhedral oligomeric silsesquioxane (POSS) molecules with varying aluminum and alkali (sodium or potassium) concentrations. Notable trends emerge from this study namely, (1) the thermodynamic stability of the substituted POSS molecules is critically dependent on the interplay between size and composition of the POSS structures, and (2) larger POSS structures provide lower central electron density and hence better accommodate the central alkali atom. These observations, when viewed in the context of aluminosilicate based geopolymers, provide fundamental insights into the relations that describe the structure composition interplay of their underlying monomers.

## Introduction

Polyhedral oligomeric silsesquioxanes (POSS)[1–3] are caged structures consisting of silicon–oxygen frameworks. Typically, POSS structures are functionalized with organic substituents to enable polymerization and/or to make them compatible with other polymers. This ability has paved way for the development of hybrid structures that have enhanced thermal, viscoelastic and chemical properties.[4–7] More recently, there has been an increasing interest in synthesizing metallo-silsesquioxanes, where a transition metal atom (such as Mo, W, Zr) replaces a silicon atom in the cage-structure.[8–11] These compounds have been identified as possible catalytic precursors for olefin polymerization.[11,12] Using these investigations as stepping stones and utilizing density functional theory (DFT), this paper examines the role of aluminum substitution (in place of silicon) and its ensuing effect on the structure and energetics of POSS cage structures. Every aluminum substitution is accompanied by the incorporation of a corresponding addition of an alkali atom (sodium or potassium) in order to ensure charge neutrality. A primary focus of this study is the characterization of the interplay between the size of the aluminum substituted POSS cage structures, and their ability to accommodate a central alkali ion within the cage as well as additional alkali ions that are required for ensuring charge neutrality for a given silicon/aluminum ratio.

On a related note, information gleaned from this study will also be examined in the context of geopolymers. Geopolymers are hydrated aluminosilicate based polymers that have very similar binding and mechanical properties of Portland cement,[13,14] with a much smaller carbon footprint due to a reduction of 80–90% in carbon emissions[15,16] during processing. Geopolymers are synthesized by activating a source material such as fly ash using aqueous alkali solutions, leading to the formation of a biphasic composite consisting of unreacted source material particles, which are bonded by a polymerized geopolymer binder phase[16] that is obtained through a condensation process.[16] Although it is known that the fully polymerized geopolymer binder phase resembles a nanoporous network of tetrahedrally coordinated aluminate and silicate units containing interstitial alkali atoms,[16] insights into the structure-composition relations of the underlying monomeric building blocks is not yet available, which will be simultaneously addressed in this work. Specifically, noting the fact that POSS molecules as well as geopolymers are characterized by tetrahedrally coordinated silicate units, and given the inherent porosity of POSS cage structures, an analysis of the aluminum substituted POSS structures should provide valuable information on the monomeric building blocks of aluminosilicate based geopolymers.

Towards the end, this work examines and provides fundamental insights into the relative energetics of simple POSS molecules [$(HSiO_{1.5})_n$; $n = 8, 10, 12$] as a function of silicon to aluminum ratio, with a corresponding alkali (sodium or potassium) counter-ion being simultaneously incorporated for every aluminum substitution. Specifically, using DFT, energy minimized structures are obtained for all considered POSS structures, and the corresponding ground-state energetics,



https://doi.org/10.1557/mrc.2015.58 Published online by Cambridge University Press

structure and Mulliken charges are analyzed to obtain quantitative trends for characterizing the interplay between cage-size and composition. Further, to emulate the composition of geopolymers' building blocks, nominally hydrated POSS structures [$(OHSiO_{1.5})_n$; $n = 8, 10, 12$] are considered and examined using the same metrics as identified above, since it is well-known that the polymerization of the geopolymers proceed via a series of condensation reactions between –OH containing monomers.[16]

## Computational methods

Calculations were performed using the quantum chemistry software package Gaussian (g09)[17] within the framework of DFT. The basis set used for all atoms was 6-311G(p,d) and additionally, the larger 6-311++G(p,d) were also used for select structures to discern the effect of the basis sets on obtained results. The exchange and correlation functional(s) used were the hybrid functional of Becke and Lee-Yang-Parr (B3LYP)[18,19] and the generalized gradient approximation of Perdew, Burke and Ernzerhoff (PBE).[20] All geometries were fully optimized in the gas phase using both B3LYP and PBE. Both PBE and B3LYP yielded very similar results and hence results using B3LYP will be presented.

In particular, the reported results in this work focus on the examination of the ground-state geometries and energies of three POSS molecules (Fig. 1) of different sizes namely $T_8$ [Fig. 1(a)], $T_{10}$ [Fig. 1(b)] and $T_{12}$ [Fig. 1(c)] as a function of Al and Na/K substitution. The calculations are restricted to silicon to aluminum ratios greater than or equal to 1:1, while examining the POSS structures, to ensure consistency with the fact that silsesquioxanes are essentially Si-based structures. The optimized structures of silicon to aluminum ratio of 1:1 for $T_8$ [Fig. 2(a)], $T_{10}$ [Fig. 2(b)] and $T_{12}$ [Fig. 2(c)] are shown in Fig. 2. Further, hydrated POSS molecules that serve as proxies for the monomeric building blocks of geopolymers are examined; these structures are obtained by replacing the –H terminal groups of POSS with –OH. Finally, when considering mono-substituted (i.e. one Al and one Na/K atom) structures, the Na/K atom is confined to be within the cage, though no such constraint is imposed for the subsequent substitutions. In order to locate the energy minimum structures for each system, the energy-represented direct inversion of the iterative subspace (GEDIIS) method as implemented within Gaussian (G09) was used.[21]

## Results and discussion

Table I provides the energy of formation of the different POSS molecules as a function of increasing Al (and Na/K) substitution.

The energy of formation ($\Delta E$) for the substitutions is calculated as:

$$\Delta E = E(Si_{n-x}Al_xNa_x/K_xO_{1.5n}H_n) + xE(Si) - E(Si_nO_{1.5n}H_n) - xE(Al) - xE(Na/K) \ldots . \quad (1)$$

where $x$ is the number of substitutions, $n = 8$, 10, or 12, $E(Si_{n-x}Al_xNa_x/K_xO_{1.5n}H_n)$ = energy of substituted POSS, $E(Si_nO_{1.5n}H_n)$ = energy of POSS, $E(Si)$ = energy of a Si atom, $E(Al)$ = energy of an Al atom and $E(Na/K)$ = energy of a Na/K atom. While the energy of POSS and substituted POSS is obtained from their respective optimized geometry, the energy of each atom is calculated using the appropriate ground state. The (positive) negative value of $\Delta E$ signifies the thermodynamic (un-)favorability for the substitution.

The most stable configurations for each POSS under study as obtained from respective geometry optimizations are consistent with previous investigations; specifically, Si—H, Si—O bond distances as well as H—Si—O, O—Si—O and Si—O—Si bond angles are very similar to those reported in previous experimental and theoretical studies.[22–27]

Table I points to the following: (i) increasing substitution of Al (and the corresponding Na/K) leads to thermodynamic favorability for the formation of all POSS structures; (ii) for $T_8$ and $T_{10}$, a minimum of three and two Al substitutions, respectively, are required before the energy of formation of the substituted POSS structure becomes lower than that of the parent molecule, while in contrast the energy of formation of the substituted $T_{12}$ structure is always lower than the parent molecule. This trend is independent of the choice of the charge

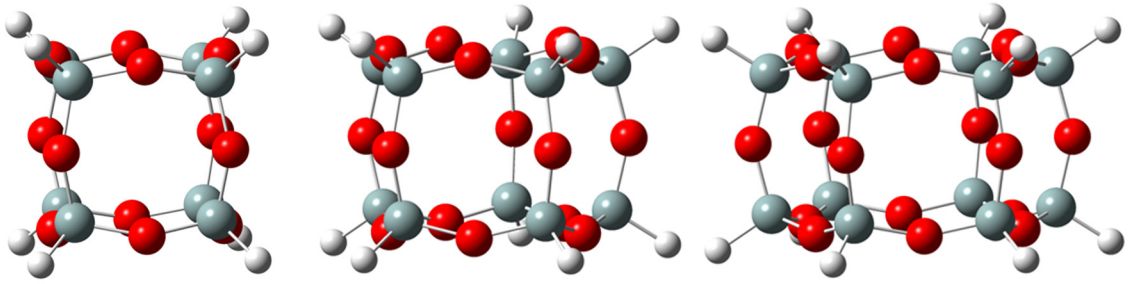



**Figure 1.** Ball and stick representation of (a) $T_8$ ($Si_8H_8O_{12}$), (b) $T_{10}$ ($Si_{10}H_{10}O_{15}$) and (c) $T_{12}$ ($Si_{12}H_{12}O_{18}$) molecules. The gray, red and white spheres represent Si, O and H atoms, respectively.


https://doi.org/10.1557/mrc.2015.58 Published online by Cambridge University Press

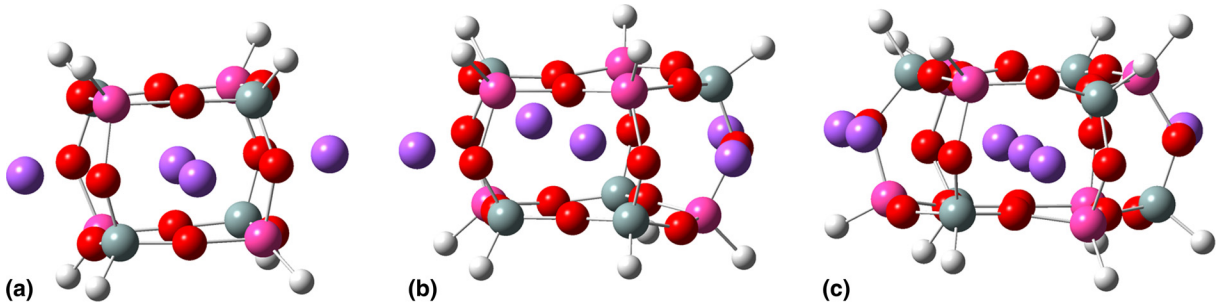



**Figure 2.** The 1:1 ratio of Si:Al in POSS molecules. (a)–(c) for $T_8$ ($Na_4Si_4Al_4H_8O_{12}$), $T_{10}$ ($Na_5Si_5Al_5H_{10}O_{15}$), and $T_{12}$ ($Na_6Si_6Al_6H_{12}O_{18}$), respectively. The pink and violet spheres represent Al and Na, respectively, and the rest of the presentation is as of Fig. 1.

compensating alkali atom; and (iii) the role of the alkali counter-ion (Na or K) on the energy of formation of the POSS structure is dependent on both the POSS cage-size and the silicon to aluminum ratio. This is evident in the preference for K over Na for $T_{12}$, and Na over K for $T_8$ and $T_{10}$ structures. In the case of the –OH substituted POSS structures (hereby denoted as $T_n$OH; $n = 8, 10, 12$), the corresponding energy of formation values are lower (i.e. more negative) with respect to the parent POSS molecules as shown in Table I. Interestingly, even for the $T_n$OH structures, increasing Al and Na/K substitution leads to further thermodynamic favorability; nevertheless, important differences in the effect of Na versus K preference is seen for the $T_n$OH structures when compared with the parent POSS molecules. Specifically, while $T_{12}$OH and $T_8$OH show preference for K and Na, respectively, for all silicon to aluminum ratios, there is a crossover point where energetically, K is preferred over Na for $T_{10}$OH structures at higher Al content. Interestingly, the role of the alkali atoms on the stability of the three different parent POSS structures we considered, is qualitatively in agreement with a previously reported investigation[28] on the stability of substituted faujasite-like rings. Of note is the fact that faujasite rings are two-dimensional in nature, while we explicitly studied three-dimensional POSS structures.

The enhancement of formation energy as a function of increasing substitution in a given POSS parent molecule is due to the fact that a single set of Si–O interactions is replaced by two sets of interactions namely Al–O, and Na(K)–O. The bond energies of Si—O and Al—O are very similar to each other. But in the substitution, an extra interaction between Na(K) and O contributes to the total binding energy and thus increases the thermodynamic favorability. If the additional substitutions favor the substitution in the POSS structures, why is it that the lower silicon to aluminum ratios fails to reflect this trend in the smaller structures? Towards the end, it is instructive to recognize that since the initial alkali atom is introduced within the POSS cage, the size of the structure should have an impact on the chemical environment of the alkali atom and consequently on the substituted structures' formation energy.

The POSS structure contains a large number of oxygen atoms whose lone pair electrons could give rise to a high electron density in the center of the structure. As the alkali atoms generally participate in chemical bonding by donation of a valence electron, it is expected that a measure of the electronic density in the region around the alkali atom would help one to understand its environment. As a measure of this electron density, the Mulliken charges on the alkali atoms for the singly substituted structures were examined.

Table II displays the Mulliken charges on alkali atoms calculated using the 6-311G** basis set used throughout this study and the 6-311++G** which adds diffuse functions to the basis set. The two basis sets yielded very similar trends with respect to formation energy of the singly substituted structures. Further, for both the cases, it is notable that the Mulliken charge on the alkali atom is *negative* for the singly substituted $T_8$, $T_8$OH, $T_{10}$, and $T_{10}$OH structures. This is indicative of a very high electron density in the center of the substituted structures and this helps to explain why these structures are less energetically favored. It is further evident that augmenting the basis set with diffuse functions serves to increase the electron density of the center of the substituted structures indicating that the smaller basis set is capable of capturing the character, but not the magnitude, of the effect of size on central electron density. By contrast, the Mulliken charges for the alkali atoms in the single substituted $T_{12}$ and $T_{12}$OH are positive showing that the large structure can better accommodate the alkali atom. This view is reinforced by the greater formation energy of the singly substituted $T_{12}$ and $T_{12}$OH structures as compared with the $T_8$ (and $T_8$OH) and $T_{10}$ (and $T_{10}$OH) systems.

Another impact of the size of the various structures can be seen by considering the relative formation energy as a function of the identity of the alkali atom. The fact that Na is preferred over K for the smaller $T_8$ and $T_{10}$ cages is a direct consequence of the larger ionic radius of K, while on the other hand, the higher electro-positivity of K coupled with the larger cage size leads to preference of K over Na for the $T_{12}$ structures. Further, it is worth noting that for all three POSS structures, with increasing alkali substitution, K provides more sequential stabilization than the sodium atom; here the sequential stabilization is defined as the difference in the formation energy of successively Al and Na/K substituted POSS structures. This



https://doi.org/10.1557/mrc.2015.58 Published online by Cambridge University Press

**Table I.** The energy of formation (kJ/mol) for the substituted POSS structures is considered in this work. A negative energy of formation indicates thermodynamic favorability of the substituted POSS molecule with respect to the parent POSS molecule.

| POSS | $T_8$ | | $T_{10}$ | | $T_{12}$ | |
|---|---|---|---|---|---|---|
| Substitution | Na | K | Na | K | Na | K |
| (a) | | | | | | |
| 1 | 112.45 | 252.61 | 7.49 | 57.89 | −94.49 | −102.26 |
| 2 | 55.08 | 180.38 | −30.14 | −37.15 | −106.57 | −132.00 |
| 3 | −41.49 | 74.29 | −105.16 | −79.96 | −146.25 | −165.00 |
| 4 | −107.79 | −16.54 | −131.14 | −112.26 | −241.50 | −277.51 |
| 5 | | | −118.23 | −114.03 | −347.39 | −358.21 |
| 6 | | | | | −383.41 | −410.78 |
| | $T_8OH$ | | $T_{10}OH$ | | $T_{12}OH$ | |
| (b) | | | | | | |
| 1 | 78.47 | 222.46 | −35.36 | 24.32 | −152.46 | −155.16 |
| 2 | 25.43 | 77.20 | −160.39 | −125.76 | −228.51 | −264.00 |
| 3 | −139.65 | −51.57 | −248.45 | −226.34 | −328.92 | −391.08 |
| 4 | −282.13 | −218.57 | −329.13 | −341.73 | −439.74 | −465.20 |
| 5 | | | −443.52 | −457.60 | −572.34 | −581.73 |
| 6 | | | | | −689.13 | −723.56 |

is attributed to the more electropositive nature of K, leading to stronger interactions with the electronegative oxygen atoms in the substituted structures as the alkali content increases. Similarly, the crossover in the $T_{10}OH$ structures can be attributed to the stronger interactions between potassium and oxygen atoms at higher K content in conjunction with the presence of terminal –OH groups.

It has been noted in the literature[29,30] that the Si—O—Al linkages are preferred to Al—O—Al linkages in zeolite frameworks and this rule is known as the Loewenstein's aluminum avoidance principle.[31] In this context, we also examined the binding energies (energy difference between system and its constituent elements) of two isomeric structures for the 50% substituted $T_8$ and $T_8OH$ structures. For a given system ($T_8$ or $T_8OH$), the structure of the respective isomers either consists of two Al—O—Al bonds or no such bonds as shown in Fig. 3. The stabilization energies (binding energy difference between pure and substituted POSS) shown in Table III establish that structures that incorporate Al—O—Al bonds exhibit less stability than those that do not (which are labeled as Si—O—Al structures) in accordance with the Loewenstein's principle. Further, the identity of the alkali atom (whether sodium or potassium) determines the scale of the stabilization energy for the 50% substituted $T_8$ and $T_8OH$ isomers.

The calculated results have provided valuable insight into the interplay between the POSS structures' size, composition, energetics and the role of aluminum (and alkali) substitution on the POSS stability. Further, the analysis of the hydrated

**Table II.** Mulliken charge on alkali atoms for POSS structures with a single substitution (Na/K+Al for one Si).

| Basis set | Alkali | $T_8$ | $T_8OH$ | $T_{10}$ | $T_{10}OH$ | $T_{12}$ | $T_{12}OH$ |
|---|---|---|---|---|---|---|---|
| 6-311G** | Na | −0.71 | −0.76 | −0.34 | −0.44 | 0.51 | 0.52 |
| | K | −0.60 | −0.73 | −0.19 | −0.29 | 0.64 | 0.67 |
| 6-311++G** | Na | −4.87 | −4.88 | −2.78 | −2.92 | 0.73 | 0.48 |
| | K | −4.55 | −4.02 | −2.42 | −2.02 | 0.93 | 0.77 |


https://doi.org/10.1557/mrc.2015.58 Published online by Cambridge University Press

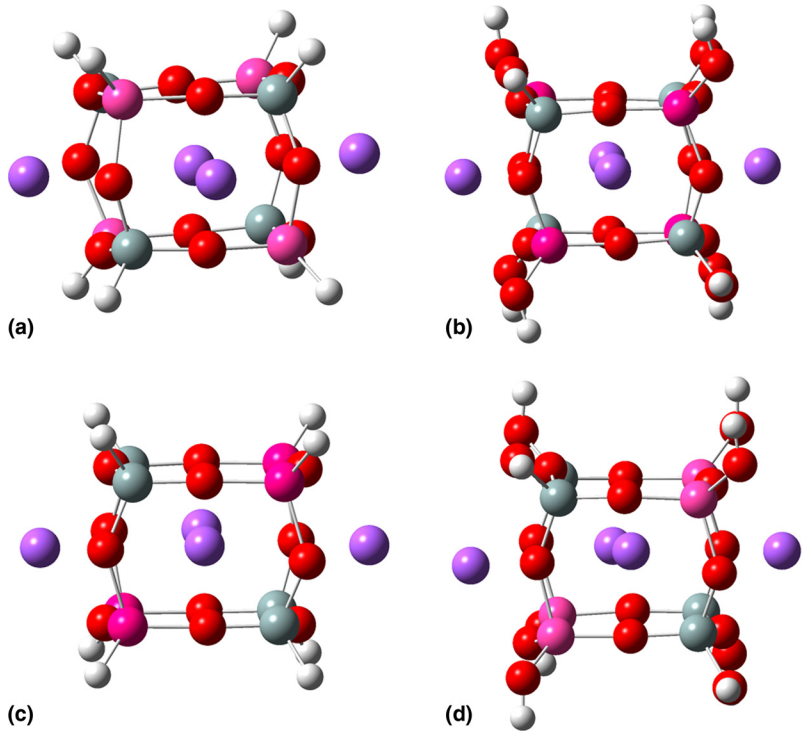



**Figure 3.** The 1:1 ratio of Si:Al in POSS molecules. (a) $T_8$ ($Na_4Si_4Al_4H_8O_{12}$) without Al—O—Al bridges, (b) $T_8OH$ ($Na_4Si_4Al_4H_8O_{20}$) without Al—O—Al bridges, (c) $T_8$ ($Na_4Si_4Al_4H_8O_{12}$) with Al—O—Al bridges and (d) $T_8OH$ ($Na_4Si_4Al_4H_8O_{20}$) with Al—O—Al bridges. The presentation is as of Fig. 2.

**Table III.** Stabilization energy (kJ/mol) for $T_8$ and $T_8OH$ structures containing either a combination of Si-O-Al and Al-O-Al linkages (row 3) or exclusively Si-O-Al linkages (row 4); the Si:Al ratio for the reported systems equal 1:1 as given in (Fig. 3).

| POSS | $T_8$ | | $T_8OH$ | |
|---|---|---|---|---|
| Substitution | Na | K | Na | K |
| Al-O-Al | −43.83 | 45.09 | −217.20 | −152.74 |
| Si-O-Al | −107.79 | −16.54 | −282.13 | −218.57 |

POSS structures has important implications for developing a fundamental understanding of the building blocks of aluminosilicate geopolymers. Specifically, our studies show that low silicon to aluminum ratios lead to better stability of the –OH terminated POSS molecules; further for a given silicon to aluminum ratio, the charge balancing alkali atoms provide higher stability to larger POSS cage structures, with the lower electron density at the middle of the larger POSS cages enabling better accommodation of the central alkali atom. These observations provide insights into the nature of the monomeric building blocks of geopolymers. It can be hypothesized that the monomers should be similar to or larger than the $T_{12}OH$ structures considered in this study in order to accommodate alkali atoms. Further, this work also provides a basis for the evaluation of various geopolymer processing options to allow the design of materials with desirable structural properties.

## Conclusion

A hybrid functional density-functional theory calculation has been carried out to examine the thermodynamics of different six POSS molecules when Si is sequentially substituted by a pair of Al and sodium or potassium atoms. Three trends are clear from the investigation:

(1) The energy of formation of substituted structures decreases (more negative) as the number of substitutions increases.
(2) From a stability point of view, for a given silicon to aluminum ratio, sodium is preferred for the $T_8$ and $T_{10}$ POSS



https://doi.org/10.1557/mrc.2015.58 Published online by Cambridge University Press

structures, while potassium is preferred for the $T_{12}$ structure.

(3) Most significantly for the design of geopolymers, the size of the monomer unit determines the suitability of formation of the substituted structure when the alkali atom is incorporated in the center of the structure. In particular, it is found that the largest of the structures that have been examined $T_{12}$ and $T_{12}OH$ are the minimal size for which the central electron density is sufficiently small to easily accommodate the alkali atom.

## Acknowledgments

The authors (A. A, K. M) would like to acknowledge financial support from NIOSH (Grant: 200-2014-59953).

## References

1. D.W. Scott: Thermal rearrangement of branched-chain methylpolysiloxanes. *J. Am. Chem. Soc.* **68**, 356 (1946).
2. Q. Zhang, H. He, K. Xi, X. Huang, X. Yu, and X. Jia: Synthesis of N-Phenylaminomethyl POSS and its utilization in polyurethane. *Macromolecules* **44**, 550 (2011).
3. S.E. Anderson, E.S. Baker, C. Mitchell, T.S. Haddad, and M.T. Bowers: Structure of hybrid polyhedral oligomeric silsesquioxane propyl methacrylate oligomers using ion mobility mass spectrometry and molecular mechanics. *Chem. Mater.* **17**, 2537 (2005).
4. F.J. Feher and D.A. Newman: Enhanced silylation reactivity of a model for silica surfaces. *J. Am. Chem. Soc.* **112**, 1931 (1990).
5. F.J. Feher, D.A. Newman, and J.F. Walzer: Silsesquioxanes as models for silica surfaces. *J. Am. Chem. Soc.* **111**, 1741 (1989).
6. N.P. Hacker: Organic and inorganic spin-on polymers for low-dielectric-constant applications. *MRS Bull.* **22**, 33 (1997).
7. C. Jin, J.D. Luttmer, D.M. Smith, and T.A. Ramos: Nanoporous silica as an ultralow-k dielectric. *MRS Bull.* **22**, 39 (1997).
8. F.J. Feher and T.L. Tajima: Synthesis of a molybdenum-containing silsesquioxane which rapidly catalyzes the metathesis of olefins. *J. Am. Chem. Soc.* **116**, 2145 (1994).
9. F.J. Feher, J.F. Walzer, and R.L. Blanski: Olefin polymerization by vanadium-containing polyhedral oligometallasilsesquioxanes. *J. Am. Chem. Soc.* **113**, 3618 (1991).
10. F.J. Feher: Polyhedral oligometallasilsesquioxanes (POMSS) as models for silica-supported transition-metal catalysts. Synthesis and characterization of (C5Me5)Zr[(Si7O12)(c-C6H11)7]. *J. Am. Chem. Soc.* **108**, 3850 (1986).
11. F.T. Edelmann: Model compounds for metal oxides on SiO2 surfaces. *Angew. Chem. Int. Ed.* **31**, 586 (1992).
12. W.A. Herrmann, R. Anwander, V. Dufaud, and W. Scherer: Molecular siloxane complexes of rare earth metals—model systems for silicate-supported catalysts? *Angew. Chem. Int. Ed.* **33**, 1285 (1994).
13. J. Davidovits: *Geopolymer Chemistry and Applications*, 3rd ed. (Institut Geopolymere, Saint-Quentin, 2011).
14. J.L. Provis and J.S.J. van Deventer: *Geopolymers: Structures, Processing, Properties and Industrial Applications* (Woodhead Publishing Limited, Cambridge, 2009).
15. P. Duxson, J.L. Provis, G.C. Lukey, and J.S.J. van Deventer: The role of inorganic polymer technology in the development of green concrete. *Cem. Concr. Res.* **37**, 1590 (2007).
16. P. Duxson, A. Fernandez-Jimenez, J.L. Provis, G.C. Lukey, A. Palomo, and J.S.J. van Deventer: Geopolymer technology: the current state of the art. *J. Mater. Sci.* **42**, 2917 (2007).
17. Gaussian 09, Revision D.01, M.J. Frisch, G.W. Trucks, H.B. Schlegel, G. E. Scuseria, M.A. Robb, J.R. Cheeseman, G. Scalmani, V. Barone, B. Mennucci, G.A. Petersson, H. Nakatsuji, M. Caricato, X. Li, H. P. Hratchian, A.F. Izmaylov, J. Bloino, G. Zheng, J.L. Sonnenberg, M. Hada, M. Ehara, K. Toyota, R. Fukuda, J. Hasegawa, M. Ishida, T. Nakajima, Y. Honda, O. Kitao, H. Nakai, T. Vreven, J.A. Montgomery Jr., J.E. Peralta, F. Ogliaro, M. Bearpark, J.J. Heyd, E. Brothers, K. N. Kudin, V.N. Staroverov, R. Kobayashi, J. Normand, K. Raghavachari, A. Rendell, J.C. Burant, S.S. Iyengar, J. Tomasi, M. Cossi, N. Rega, J. M. Millam, M. Klene, J.E. Knox, J.B. Cross, V. Bakken, C. Adamo, J. Jaramillo, R. Gomperts, R.E. Stratmann, O. Yazyev, A.J. Austin, R. Cammi, C. Pomelli, J.W. Ochterski, R.L. Martin, K. Morokuma, V. G. Zakrzewski, G.A. Voth, P. Salvador, J.J. Dannenberg, S. Dapprich, A. D. Daniels, Ö. Farkas, J.B. Foresman, J.V. Ortiz, J. Cioslowski, and D. J. Fox: (Gaussian, Inc., Wallingford, CT, 2009).
18. A.D. Becke: Density-functional thermochemistry. III. The role of exact exchange. *J. Chem. Phys.* **98**, 5648 (1993).
19. C.T. Lee, W.T. Yang, and R.G. Parr: Development of the Colle-Salvetti correlation-energy formula into a functional of the electron density. *Phys. Rev. B* **37**, 785 (1988).
20. J.P. Perdew, K. Burke, and M. Ernzerhof: Generalized gradient approximation made simple. *Phys. Rev. Lett.* **77**, 3865 (1996).
21. X. Li and M.J. Frisch: Energy-represented DIIS within a hybrid geometry optimization method. *J. Chem. Theory Comput.* **2**, 835 (2006).
22. T. Baudilio and M.S. Gordon: Insertion mechanism of $N_2$ and $O_2$ into $T_n(n = 8, 10, 12)$-silsesquioxane Framework. *J. Phys. Chem. B* **106**, 11764 (2002).
23. K.W. Törnroos: Structure of octahydridosilasesquioxane determined by neutron diffraction. *Acta Cryst.* **C50**, 1646 (1994).
24. K.-H. Xiang, R. Pandey, U.C. Pernisz, and C. Freeman: Theoretical study of structural and electronic properties of H-silsesquioxanes. *J. Phys. Chem. B* **102**, 8704 (1998).
25. C.W. Earley: A quantum mechanical investigation of silsesquioxane cages. *J. Phys. Chem.* **98**, 8693 (1994).
26. T.P.E. Heyde, H.-B. Bürgi, H. Bürgi, and K.W. Törnroos: The crystal and molecular structure of the symmetrical silasesquioxane $H_8Si_8O_{12}$ at 100 K, a molecular building block of some zeolites. *Chimica* **45**, 38 (1991).
27. K.W. Törnroos, H.-B. Bürgi, G. Calzaferri, and H. Bürgy: The crystal and molecular structure of dodecahydridosilasesquioxane, $H_{12}Si_{12}O_{18}$. *Acta Cryst.* **B51**, 155 (1995).
28. C. Gatti, G. Ottonello, and P. Richet: Energetics and bonding in aluminosilicate rings with alkali metal and alkaline-earth metal charge-compensating cations. *J. Phys. Chem. A* **116**, 8584 (2012).
29. Y. Xiang, J. Du, M.M. Smedskjaer, and J.C. Mauro: Structure and properties of sodium aluminosilicate glasses from molecular dynamics simulations. *J. Chem. Phys.* **139**, 044507 (2013).
30. M. Bauchy: Structural, vibrational, and elastic properties of a calcium aluminosilicate glass from molecular dynamics simulations: the role of the potential. *J. Chem. Phys.* **141**, 024507 (2014).
31. W. Loewenstein: The distribution of aluminum in the tetrahedra of silicates and aluminate. *Am. Mineral.* **39**, 92 (1954).


https://doi.org/10.1557/mrc.2015.58 Published online by Cambridge University Press